

# VERDI: Versatile diffractometer with wide-angle polarization analysis for magnetic structure studies in powders and single crystals

V. Ovidiu Garlea,<sup>1, a)</sup> Stuart Calder,<sup>1, b)</sup> Thomas Heugle,<sup>2</sup> Jiao Lin,<sup>3</sup> Fahima Islam,<sup>2</sup> Alexandru Stoica,<sup>1</sup> Van B. Graves,<sup>3</sup> Benjamin Frandsen,<sup>4</sup> and Stephen Wilson<sup>5</sup>

<sup>1)</sup>*Neutron Scattering Division, Oak Ridge National Laboratory, Oak Ridge, TN 37831, USA*

<sup>2)</sup>*Neutron Technology Division, Oak Ridge National Laboratory, Oak Ridge, TN 37831, USA*

<sup>3)</sup>*Second Target Station, Oak Ridge National Laboratory, Oak Ridge, TN 37831, USA*

<sup>4)</sup>*Department of Physics and Astronomy, Brigham Young University, Provo, UT 84602, USA*

<sup>5)</sup>*Materials Department and California Nanosystems Institute, University of California Santa Barbara, Santa Barbara, CA 93106, USA*

(Dated: 3 March 2022)

The VERDI diffractometer will set a new standard for a world-class magnetic diffractometer with versatility for both powder and single crystal samples and capability for wide-angle polarization analysis. The instrument will utilize a large single-frame bandwidth and will offer high-resolution at low momentum transfers and excellent signal-to-noise ratio. A horizontal elliptical mirror concept with interchangeable guide pieces will provide high flexibility in beam divergence to allow for either a high-resolution powder mode, a high-intensity single crystal mode, and a polarized beam option. A major science focus will be quantum materials that exhibit emergent properties arising from collective effects in condensed matter. The unique use of polarized neutrons to isolate the magnetic signature will provide optimal experimental input to state-of-the-art modeling approaches to enable detailed insight into local magnetic ordering.

## I. INTRODUCTION

Neutron diffraction is the premier technique to determine the nature of magnetic short- and long-range ordering of materials due to the well understood neutron scattering cross section. The ever increasing complexity of magnetic systems, which often involve coupled spin, orbital, and lattice degrees of freedom, calls for much improved instrumentation that provides high resolution at low- $Q$ , high intensity, reduced extrinsic background and polarization analysis capability. The VERDI diffractometer is designed to take full advantage of the high brightness and wide energy bandwidth offered by the Second Target Station (STS) at the Spallation Neutron Source (SNS) and will provide transformative capabilities for the research involving magnetism and spintronics.

In the context of the neutron suite at ORNL, VERDI will be unique in being a wide-wavelength bandwidth diffractometer optimized for magnetic studies at a variety of sample environment conditions and fill a clear gap in current capabilities at SNS first target station (FST) and HFIR.<sup>1</sup> All current or planned SNS diffractometers that are situated at the FTS make use of a narrow bandwidth at short wavelengths for their science focus. This naturally limits the low  $Q$  capabilities possible. Instruments at HFIR currently offer options for magnetic structure determination; however, they have limited  $Q$ -range and

resolution. Therefore, VERDI will greatly complement the current oversubscribed diffraction suite at ORNL by offering longer wavelengths, lower background, full polarization analysis and higher resolution to tackle more complex science problems not feasible on the current instrumentation. Considering other neutron facilities, the WISH<sup>2</sup> instrument located at ISIS-TS2 is the most analogous instrument in current operation worldwide and is widely considered the world-leading powder diffractometer for magnetic studies. The operating frequencies of ISIS-TS2 (10 Hz) and SNS-ST5 (15 Hz) are similar; however, the peak brightness at the ST5 allows VERDI significant flux gains compared to WISH. As shown from simulations shown in Fig. 1, VERDI will have an order of magnitude increased flux on sample compared to WISH.

A major science focus at VERDI will be quantum materials that exhibit emergent properties arising from collective effects in condensed matter. Materials with strong spin-orbit coupling and even modest electron-electron correlation effects have recently been identified to manifest a host of novel new electronic states.<sup>3-6</sup> These include spin-orbit entangled Mott insulators, Kitaev spin liquids, and correlated topological materials. Limitations in elucidating the magnetic ground states of these systems lie in the fast decaying magnetic form factors associated with the extended nature of the magnetic orbitals (typically  $4d$  or  $5d$  electron), the weak intrinsic moments in these materials, and the small sample volumes from synthesis or neutron absorption constraints. These challenges highlights the critical need for a high-flux and low background VERDI instrument that can probe small sample crystal sizes and powder sample vol-

---

<sup>a)</sup>Electronic mail: garleao@ornl.gov

<sup>b)</sup>Electronic mail: caldersa@ornl.gov

umes (milligrams) with small ( $<0.2\mu_B$ ) or dilute ordered moments. Such measurements should additionally be feasible in pressure cells, requiring tunable beam sizes.

Unique opportunities also exist in the field of energy material research from superconductors to thermoelectrics and multiferroics.<sup>7,8</sup> Due to its high resolution at low- $Q$  and ability to precisely define magnetic reflections, VERDI will be a leading tool for probing complex incommensurate and multi- $Q$  magnetic structures within extreme sample environments. Additionally, polarization analysis will provide a powerful tool to probe and distinguish between intertwined degrees of freedom and to unambiguously resolve the nature of the driving noncoplanar, often incommensurate magnetic orders.

VERDI will also unlock the potential of magnetic hybrid materials due to its ability to study their magnetism, where spins are typically dispersed over organic linkers.<sup>9,10</sup> This requires polarization measurements to reveal the spin interaction, direction, and location through magnetization density plots. Additionally, the large unit cell size and complex interaction pathways usually present within organic magnets results in long-wavelength incommensurate structures,<sup>11</sup> necessitating high  $Q$ -resolution. Furthermore, the strong magneto-coupling inherent in these materials and the ability to combine magnetism with tailored properties from organic linkers will require simultaneous understanding of both the spin and lattice, requiring the wide  $Q$ -coverage with the superior resolution promised by VERDI. The implementation of polarization also allows the isolation of the incoherent scattering, which offers advantages when studying hydrogen-based materials.

Magnetic diffuse scattering analysis in both powders and crystals has recently emerged as a powerful tool for investigating short-range magnetic interactions and correlations at the nanoscale.<sup>12–15</sup> Such effects are important in diverse materials classes, including quantum materials, energy conversion materials, and spintronics such as dilute magnetic semiconductors. The greatest obstacles in conducting magnetic diffuse scattering analysis are accurately measuring the magnetic diffuse-scattering signal over a wide range of momentum transfer and separating magnetic from nonmagnetic scattering. In a typical magnetic diffuse-scattering experiment, the magnetic scattering is collected together with the nuclear scattering, which is usually much stronger. The natural solution is to perform wide-angle polarization analysis to separate the magnetic and nuclear scattering. Unfortunately, existing instruments with this capability provide only a limited range of momentum transfer. VERDI instrument will revolutionize magnetic diffuse-scattering studies by offering polarization analysis capability across a wide range of momentum transfer – between 0.1 and 8  $\text{\AA}^{-1}$  to isolate the magnetic scattering for both powder and single-crystal samples.

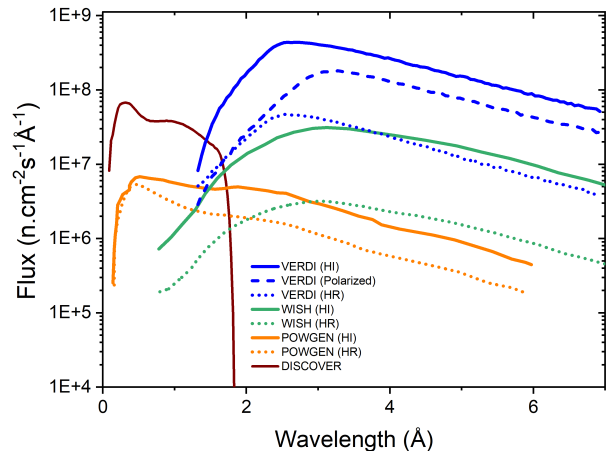


FIG. 1. Flux at sample position against wavelength comparing VERDI (STS), WISH (ISIS-TS2), POWGEN (SNS) and DISCOVER (SNS).

## II. SCIENCE DRIVEN CAPABILITIES REQUIREMENTS

The overriding scientific driver for VERDI is to probe magnetic order in powders and single crystals. The emphasis, therefore, is on offering high resolution at low momentum transfers, which can be traded for higher flux as required, with a low background. Full polarization capabilities is a key science driver. Flexibility in beam divergence is required to allow measurements of both powder and single crystals, as well as different sample sizes. The high-level capability requirements derived from science goals are detailed below and summarized in Table I.

i) *Optimized range of momentum space*: VERDI requires the use of cold neutrons to access the required  $Q_{min} \approx 0.1 \text{ \AA}^{-1}$  ( $d \approx 65 \text{ \AA}$ ). On the other hand, a large  $Q$ -range is still necessary for most of the anticipated science. For example, magnetic PDF studies need access to both low  $Q$  as well as a  $Q_{max} \approx 7\text{-}8 \text{ \AA}^{-1}$ . To provide the necessary  $Q$ -range in a single wavelength band, a wide bandwidth is required, combined with wide detector coverage.

ii) *High resolution*: Resolution of  $\Delta Q/Q \approx 0.3\%$  is required to investigate complex magnetism, such as incommensurate magnetic structures. The resolution will be variable to allow high resolution and high flux modes as required.

iii) *Low background*: Excellent signal-to-noise ratio is crucial to investigate small magnetic signals and/or milligram-size samples and is a central consideration driving all aspects of the instrument design. This has led to the consideration of a curved guide layout to avoid a direct line of sight to the moderator and mitigate background from fast neutrons and radiation.

iii) *Wide-angle polarization analysis*: The polarization of the incident beam and analysis of scattered beam needs to be automated and to be switched in a simple

TABLE I. Key capability requirements for VERDI.

Parameter	Description
Beam size at sample	5 x 5 mm <sup>2</sup> to 10 x 10 mm <sup>2</sup>
Beam divergence	
High resolution:	0.2° (Hor), 1° (Vert)
High intensity:	1° (H), 1° (V)
Q-range	0.1 Å <sup>-1</sup> ≤ Q ≤ 9 Å <sup>-1</sup>
Q-resolution	ΔQ/Q ≈ 0.3%
Bandwidth (Δλ)	6 Å (15 Hz)
Polarization	wide-angle polarization analysis
Sample environment	sample changer, mili-Kelvin T, magnetic fields, pressure

“push-button” fashion between polarized and unpolarized modes. For this, it is planned to use a wide-angle supermirror analyzer, similar to the one used at the HYSPEC<sup>16</sup> instrument at SNS. This flexibility will allow achieving a balance between more specialized polarized measurements and workhorse unpolarized mail-in-type experiments.

iv) *Variable beam divergence*: Both powders and single crystals will be measured. To accommodate the different sample sizes a variable beam size from 5 by 5 mm (crystals) to 10 by 10 mm (powders) will be needed. Therefore, the beam divergence will need to be variable: 0.2–1° horizontal and 1° vertical for powders (High Resolution) and symmetric of ≈ 1° for single crystals (High Intensity).

v) *Large detector coverage*: To measure both powders and single crystals, a large horizontal detector coverage, covering 320° (2 x 160°), is needed for the wide Q-range. For single crystal measurements, continuous detector coverage and sufficient out-of-plane coverage is required. The detectors must be able to operate in the presence of stray magnetic fields.

vi) *Broad range of sample environment*: Dilution temperatures, magnetic fields, and pressure measurements are expected to be routine; therefore, the sample area should be able to accommodate them. Sample translation and centering capabilities will be incorporated. Automated multi-sample changer options for sample environments will be developed to efficiently utilize the high beam flux. A dedicated magnet for fields 14 T with optimized out-of-plane coverage is anticipated to satisfy the science cases for measuring magnetic structures in applied fields.

### III. PHYSICS DESIGN AND ENGINEERING CONCEPT

VERDI is planned to be located at the ST13 beam-line positions of STS and will face the cylinder coupled para-hydrogen moderator with a 3 by 3 cm<sup>2</sup> viewed area. Monte Carlo simulations using the McStas package<sup>17</sup> have been performed to inform the VERDI design and ensure that the instrument achieves the science-driven key

instrument capabilities. The optimal moderator–sample instrument length, based on McStas simulations, is 40 m. The engineering concept of VERDI and a schematic of key instrument components is displayed in Fig. 2. Table II lists the main instrument components and their positions along the beam line.

#### A. Guide

A curved/deflected guide layout, shown in Fig. 2, as opposed to a guide providing a direct view of the moderator, offers the lowest-background option and therefore fulfills a key science-driven requirement. This choice cuts off wavelengths below 1 Å; however, it will not compromise the science-driven  $Q_{max} \approx 8 \text{ \AA}^{-1}$  or required bandwidth. The VERDI horizontal elliptical mirror concept allows for both a high-resolution powder mode, a high-intensity single crystal mode, and a polarized beam option with interchangeable guide pieces. The first guide is the same for all modes. It starts at 6.35 m at an initial displacement of 84 mm and ends at 26.9 m with a displacement of 75.5 mm off axis, illuminating a secondary source at 31.75 m. The ellipse is defined by  $y = 2b \cdot \sqrt{\frac{x}{L} \cdot (1 - \frac{x}{L})}$ , where  $b$  is the semi minor axis (10.5 cm),  $x$  is the coordinate along the beam, and  $L$  (the major axis of the ellipse) is the distance between the moderator and the secondary source: 31.75 m. An adjustable slits system will allow for a fine definition of the secondary source size. Three different mirrors can be moved into place after the secondary source by means of a translation table: (1) A high resolution option with an elliptical mirror starting at 32.93 m with a displacement of -17.5 mm at the entrance. The exit is at 36.46 m, displaced by -24.74 mm ( $b = 2.5$  cm). (2) A high intensity option with an elliptical mirror starting at 35.05 m, displaced by -49 mm, and ending at 37.5 m with an exit displacement of -18.37 mm ( $b = 5$  cm). (3) Finally, a polarizing supermirror of the same shape as the high intensity option described. The major axis of the ellipse is 8.25 m for all three cases. A supermirror ratio of  $m = 3.6$  would be enough to secure reflection of neutrons over a 1 Å wavelength for polarized operation.

The overall shape of the vertical guide is an ellipse with a semi-minor axis of 19.78 m and a semi-major axis of 18.06 m. Since the vertical guide attaches to the horizontal counterparts described above, it has several interruptions that cause gaps. The individual guide pieces are therefore slightly offset against each other to prevent holes in the sample illumination. The ellipse is coupled with a feeder guide (1.27 m long) starting at 6.18 m and tapering in width from 2.38 cm to 2.4 cm.

The neutron optics system described above was modeled using the McStas package<sup>17</sup> to generate an estimate of performance for two modes of operation, high-resolution powder samples and high-intensity single crystal samples. For powder measurements, the beam is defined by slits of 11 by 11 mm<sup>2</sup> and divergence of 0.23°

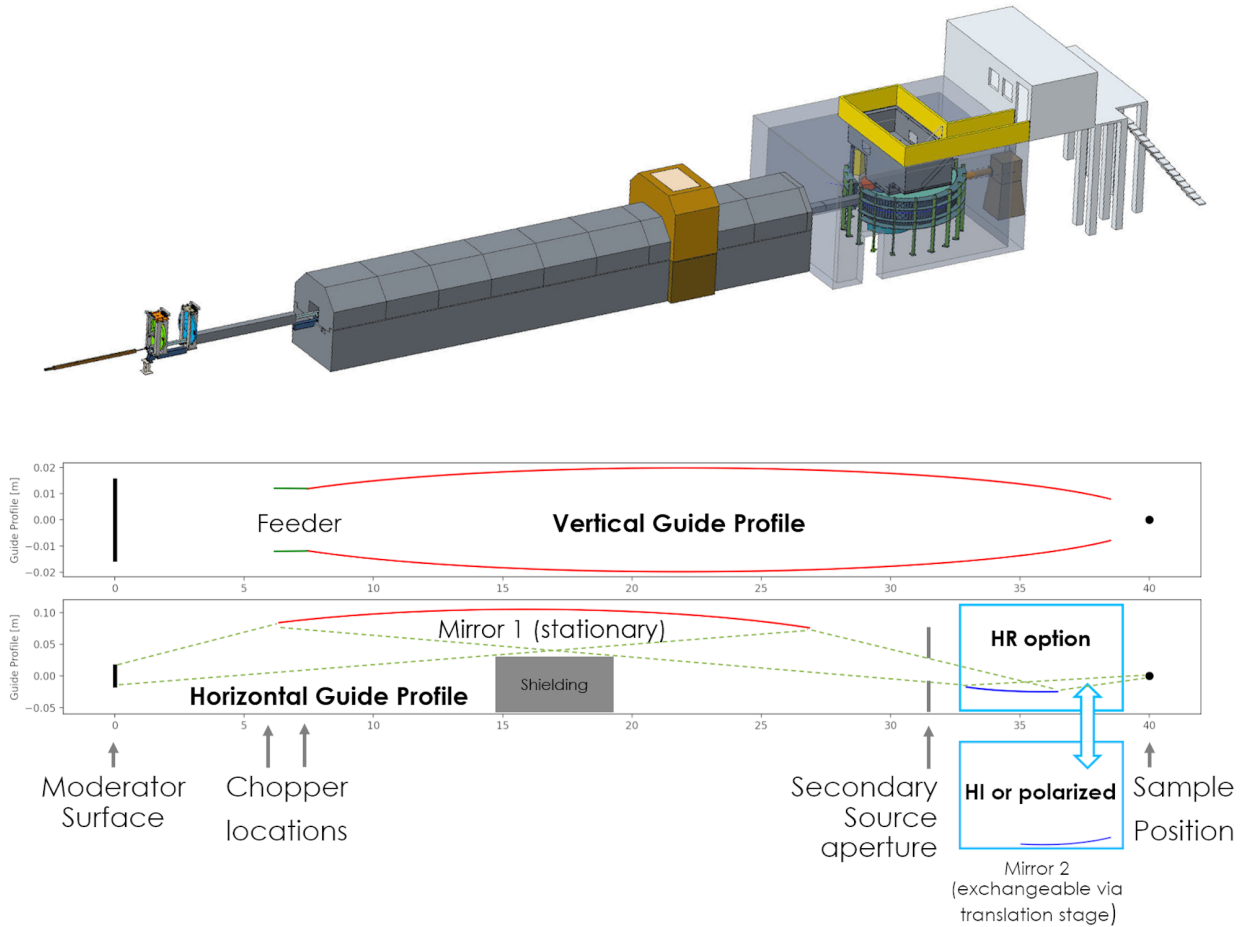


FIG. 2. Engineering concept of VERDI (top) and schematic of curved guide layout (bottom). The main instrument components are indicated on the x axis. The vertical guide profile is identical for all measurement modes. The horizontal guide profile consists of a long first mirror illuminating a secondary source, from where the beam is transported by three interchangeable guide options: High Resolution (HR), High Intensity (HI), and a polarized supermirror whose shape matches that of the HI option.

(FWHM). For single crystal measurements, the beam is 5 by 5 mm<sup>2</sup> with a divergence of 0.9° (FWHM). The peak flux for high-resolution powder mode is  $4.77 \times 10^7$  n/s/cm<sup>2</sup>/Å and for high-intensity single crystal mode is  $4.35 \times 10^8$  n/s/cm<sup>2</sup>/Å. These guides offer the required neutron beam sizes and angular divergences for both modes.

VERDI guide has also been the subject of a study on the impact of guide misalignment during the STS physical installation and subsequent resettlement of the instruments over time common to all construction projects. The most significant impact is found to come from “systematic” vertical misalignment (ground settlement). A “systematic” misalignment profile with maximum offset < 1 mm would not adversely impact the flux of the instrument. Further studies on misalignments on the divergence and displacement of the beam is underway.

## B. Choppers

Two choppers (shown in Fig. 2) will be located at 6 m (double disc, C1) and 7.5 m (single disc, C2), to define the bandwidth and suppress band overlap, informed by McStas simulations. An additional (double disc) chopper at 30 m was considered but found to have negligible benefits to the instrument performance. With these chopper locations and the 40 m distance from the moderator to the sample, VERDI has an operating wavelength range of 1 to 6.75 Å with a central wavelength of 3.9 Å. Operating in frame-suppression mode at 7.5 Hz would enable the instrument to collect data from neutron wavelengths of 1 Å to 12.3 Å in a single instrument configuration as indicated in Fig. 3.

In addition to bandwidth neutron choppers, the instrument is envisioned as incorporating an optional Fermi chopper that can be translated into and out of the beam to provide a monochromatic beam. Energy analysis can

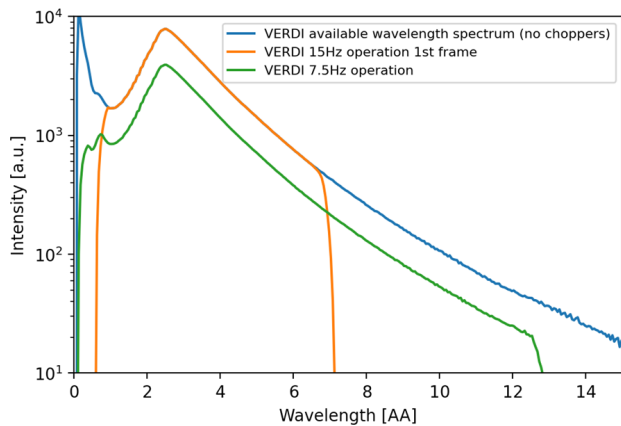


FIG. 3. Simulations of the wavelength bandwidth defined by the neutron choppers.

be beneficial for separating the weak elastic scattering in diffuse scattering measurements when inelastic fluctuations are comparable in strength. Furthermore, the monochromatic beam can help to eliminate unwanted spurious scattering from sample environments (magnet, or pressure cell) while operating the instrument in unpolarized mode.

### C. Sample area

The sample area consists of a top-loading vacuum tank with dimensions adequate to support a full set of sample environments as well as Helmholtz coils around the sample position, which will be used during measurements with polarized neutron beam. An oscillating radial collimator composed of Mylar blades will define a small sample volume, an  $\sim 15$  mm radius cylinder that the detectors will view to minimize background from non-sample scattering. This will be interchangeable with a solid angle polarizing supermirror array on one side of the instrument. The other side will have a fixed oscillating radial collimator with high out-of-plane coverage. The curved analyzer will be located on an elevator, enabling easy user selection between it and the oscillating radial collimator during measurements. A curved supermirror analyzer with  $60^\circ$  in-plane and  $\pm 7^\circ$  out-of-plane coverage is operational on HYSPEC at the SNS.<sup>16</sup> Consequently, it is anticipated that more than one analyzer could be required to achieve full angular coverage on VERDI. Out-of-plane coverage will be increased to  $\pm 13^\circ$ . The analyzer housing will be masked between the multiple modules. This will not cause any gaps in the powder data due to the wide wavelength range. For single crystal measurements it will be negated with sample rotation, with which will be performed routinely, even in unpolarized mode. To ensure reliability and ease of troubleshooting, the current concept has the collimator/analyzer in air between the vacuum tank and an argon-filled tank filling the re-

maining volume out to the detectors. Key considerations include the thickness of the windows on the argon tank. Additional options will be explored during preliminary engineering design. The detectors will be in air, allowing ease of access.

### D. Detectors

Instrument performance was compared for a logarithmic spiral detector geometry with varying sample-to-detector distance (3.1 m at  $5^\circ$  forward scattering and 1.2 m at  $165^\circ$ ) backscattering to a cylindrical geometry with detectors at a constant radius (2.5 m radius). McStas simulations were performed for various moderator-sample (L1) lengths (30 – 60 m) and approximated source divergences ( $0.1^\circ$  -  $1.0^\circ$ ). The resulting output was plotted in “onion-plots”, concentric pixelated detector rings starting from 1 m from the sample out to 4 m as a convenient way to interpret the change in resolution. The details of this simulation approach used for optimizing design parameters are given in Ref. 18. Results indicate that the spiral layout offers resolution advantages at low  $Q$ , supporting the science needs, with a smaller impact of decreased resolution in backscattering compared to a cylindrical layout.

It is planned that both sides of the instrument will have full detector coverage in the scattering plane (horizontal angular range of  $5^\circ$  to  $165^\circ$ ). However, given the anticipated cost associated with the curved polarizing supermirror analyzer, only one side will offer full polarization analysis, see Fig.4. In addition to full horizontal in-plane angular coverage, the other side of the instrument will add out-of-plane coverage over a horizontal angular range of  $45$ – $135^\circ$  from a second row of detectors (Fig. 4). This will provide additional out-of-plane coverage to enable more efficient single-crystal measurements.  $^3\text{He}$  detector tubes are the preferred detector technology because they can offer the required full gapless coverage, pixel size, compatibility with stray fields, and gamma discrimination. These are a proven technology and so represent minimal unknown risks; however, as technology advances, further options for detectors will be considered.  $^3\text{He}$  tubes 1 m tall will give suitable out-of-plane coverage of  $\simeq \pm 13^\circ$ , which will increase to  $+35^\circ$  upon the addition of an out-of-plane row, as discussed earlier. Tube diameters of 8 mm or 12.7 mm (0.5 in.) are under consideration. McStats simulations show small but observable resolution gain for 8 mm cylindrical layout detectors. Final selection will be based on the results of more detailed simulations and consideration of the increased cost associated with the smaller diameter. The inefficiencies at the edges of the tubes will potentially impact single crystal measurements; however, most measurements will be performed at several crystal rotations, which should mitigate the issue.

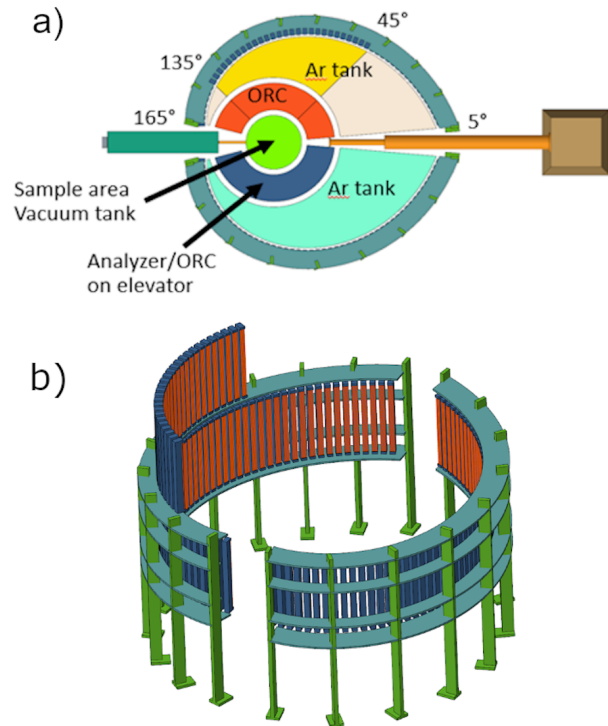


FIG. 4. Sample-detector area for VERDI. (a) Top-view of the detector with all components shown. ORC refers to the oscillating radial collimator. (b) Detector layout highlighting the spiral geometry, two-sided horizontal coverage and out of plane second row.

TABLE II. Technical parameters of VERDI diffractometer.

3.3in Moderator	Coupled hydrogen moderators
Source frequency	15 Hz at 0.7 MW
Integrated flux ( $n\text{ cm}^{-2}\text{ s}^{-1}$ )	$1.1 \times 10^9$ (High Int.) $1.1 \times 10^8$ (High Res.)
Flight Path	L1 = 40 m , L2 = 1.2 - 3.1 m
Beam size	3-10 mm variable
Peak flux wavelength	3.9 Å
Wavelength band	1 - 7 Å
Detector type/layout	logarithmic spiral $^3\text{He}$ tubes from 1.2 to 3.1m
Detector coverage	$5^\circ$ - $165^\circ$ (Hor.) $\pm 15^\circ$ (Vert)- polarized $34^\circ$ (Vert) - unpolarized
Polarization	Polarization analysis with wide-angle supermirror

#### IV. SIMULATED SAMPLE SCATTERING FROM VERDI

This section underlines some of the important experimental gains from using VERDI instrument. The scattering from a 5 mm Vanadium annular rod has been modeled using the McVine package<sup>19,20</sup> to provide a clearer picture of the accessible  $Q$  range from different experi-

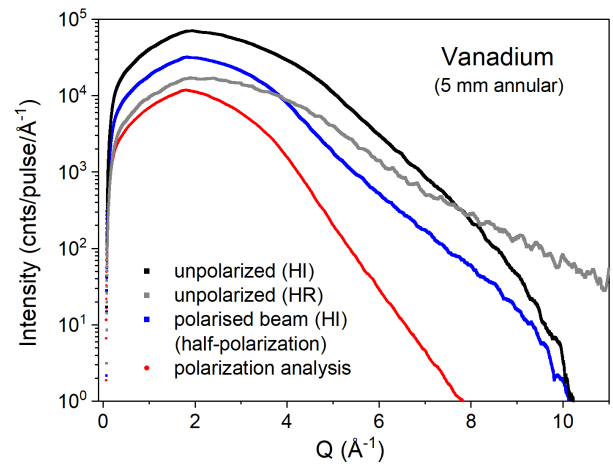


FIG. 5. Simulated scattering from a 5mm annular vanadium rod for different experimental conditions. Simulations are performed using McVine.

mental settings. As visible in Fig. 5, when operated at 15 Hz the instrument is expected to cover a momentum transfer as low as  $0.12\text{ \AA}^{-1}$  and up to  $9\text{ \AA}^{-1}$  for the high-intensity/single crystal more or even higher for the high-resolution/powder mode. Considering the low intrinsic background expected for this instrument due to the curved guide shape, full polarization analysis studies can be performed for  $Q$  range  $0.12\text{ \AA}^{-1} - 7.5\text{ \AA}^{-1}$ , if one assumes using a  $m = 3$  supermirror analyzer, similar to the one currently in use at HYSPEC<sup>16</sup>, and the polarizing supermirror located close to the sample at the high-intensity position. Further increase in the  $Q$  range for polarization analysis can be accomplished by positioning the polarizing mirror further from the sample position at the high-resolution configuration.

#### A. Powder diffraction measurements performed in high-resolution configuration

To demonstrate the importance of accessing low momentum-transfer region we simulated the magnetic Bragg scattering from a noncollinear antiferromagnetic state in the frustrated spin-chain material  $\text{NaCo}_2(\text{SeO}_3)_2(\text{OH})$ ,<sup>21</sup> that was previously investigated using the HB2A powder diffractometer at HFIR. The material orders magnetically in a two-step sequence with the wave-vectors  $k_1=(0,0,0)$  and  $k_2=(1/2,0,0)$ . The lowest magnetic peak position at about  $0.23\text{ \AA}^{-1}$  is hardly accessible when using a conventional thermal neutron diffractometer due to an appreciable background from the direct beam and poor angular resolution. Incomplete information on the magnetic scattering precludes an accurate determination of the magnetic structure. As illustrated in Fig. 6(a), this issue is overcome at VERDI where magnetic Bragg peaks can be measured down to  $0.12\text{ \AA}^{-1}$  with very good  $Q$  resolution and low background noise.

Furthermore, our Monte Carlo simulations indicate that refinable magnetic diffraction data can be obtained in 1 minute on 50 mg polycrystalline sample, which is an unprecedented performance.

The instrument's high-resolution is particularly important when dealing with incommensurate magnetic structures, such as that reported for the polar tetragonal intermetallic  $\text{NdCoGe}_3$ .<sup>22</sup> The ground state magnetic order in this material is incommensurate in all crystallographic directions with the propagation vector  $k = (0.494, 0.0044, 0.385)$ . The propagation vector was confirmed using single-crystal measurements and the magnetic structure was modeled from powder diffraction data measured POWGEN.<sup>22</sup> A unique determination of the magnetic structure was not possible, and several solutions including single or multiple- $k$  structures have been proposed. The POWGEN data, represented by red open circle symbol in Fig.6(b), does not provide sufficient signal to noise ratio and  $Q$ -resolution making it challenging to distinguish between possible spin configurations. The simulated diffraction profile for VERDI in the high-resolution mode demonstrates the improved  $Q$  resolution in the low- $Q$  region ( $< 2 \text{ \AA}^{-1}$ ) compared to the POWGEN data, which allows to clearly separate nearby magnetic reflections for more accurate Rietveld refinements. It is also noteworthy that the estimated increase in flux by about two order of magnitude at long wavelength will make such measurements statistically significant in a much shorter counting time, or from smaller samples.

## B. Magnetic PDF performed using the XYZ polarization analysis in high-intensity configuration

VERDI will revolutionize the magnetic PDF (mPDF) technique<sup>13</sup> by allowing routine collection of clean diffraction patterns with significantly improved real-space resolution than is currently attainable. These advances are made possible by the combination of full polarization analysis and the large accessible  $Q$  range of  $0.12 - 7.2 \text{ \AA}^{-1}$ , where this upper limit is a conservative estimate of what can be realistically achieved at VERDI using the high intensity configuration. Currently, the maximum available  $Q$  on an instrument with full polarization analysis is about  $5.5 \text{ \AA}^{-1}$  at HYSPEC. To illustrate the improved real-space resolution resulting from the expanded  $Q$  range at VERDI, Fig. 7 displays the mPDF pattern for the topological non-collinear antiferromagnet  $\text{Mn}_3\text{Sn}$ <sup>23</sup> generated from simulated diffraction data with different values of the maximum momentum transfer  $Q_{max}$ . Many of the fine features seen in the idealized mPDF pattern (gray dashed curved, corresponding to an infinite momentum transfer range) are lost for  $Q_{max} = 5.5 \text{ \AA}^{-1}$  (blue curve), but are at least partially recovered for  $Q_{max} = 7.2 \text{ \AA}^{-1}$  (orange curve). Sensitivity to these details in the mPDF pattern is crucial for resolving the local magnetic correlations in nontrivial spin structures such as the non-collinear magnetic structure of  $\text{Mn}_3\text{Sn}$ .

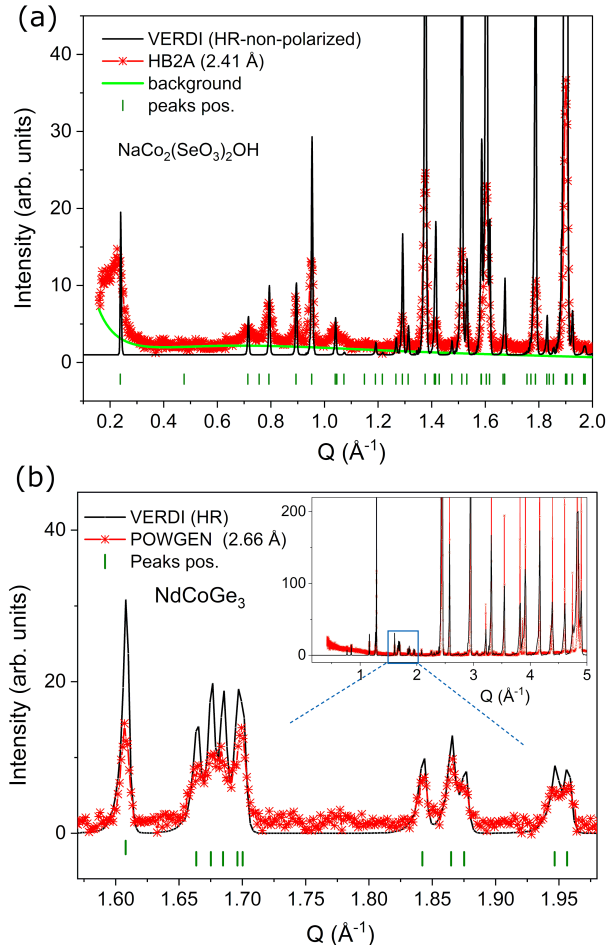


FIG. 6. Comparison of low- $Q$  coverage and  $Q$ -resolution of VERDI with HB2A (a) and POWGEN (b) instruments for two case studies involving magnetic orders with large magnetic unit cells or incommensurate propagation vectors. The relative intensities between different datasets are not reflecting the actual counting rates but are scaled for an easy comparison of the peak profiles.

We also note that mPDF data can also be obtained at dedicated total scattering instruments such as NOMAD at SNS where a much larger  $Q$  range is available. However, these instruments lack polarization analysis capabilities, hindering efforts to cleanly separate the magnetic scattering from the nuclear scattering. As a result, the effects of the magnetic form factor typically cannot be deconvoluted from the data, and the mPDF patterns obtained from such instruments suffer a large reduction in real-space resolution.<sup>13</sup> Another problem is the lack of low- $Q$  coverage at most total scattering instruments, where typical minimum  $Q$  values of  $0.5 - 1 \text{ \AA}^{-1}$  often exclude important magnetic scattering intensity at lower  $Q$ , making it impossible to obtain an accurate real-space mPDF pattern. VERDI overcomes both problems by offering polarization analysis and extending the available  $Q$  range to smaller momentum transfers. We note that

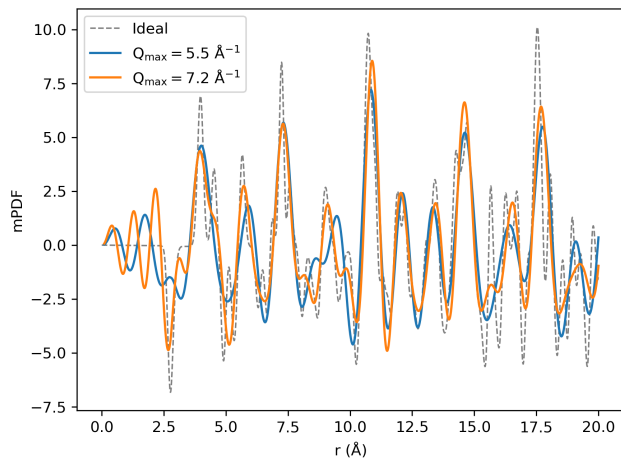


FIG. 7. Simulated mPDF patterns from a non-collinear anti-ferromagnetic state in  $\text{Mn}_3\text{Sn}$  using various maximum values of  $Q$ . The idealized mPDF pattern corresponding to an infinite momentum transfer range is shown by the gray dashed curved. The fine features are lost for  $Q_{\text{max}} = 5.5 \text{ \AA}^{-1}$  (blue curve) that is currently achievable by polarization analysis, but are mostly recovered for a  $Q_{\text{max}} = 7.2 \text{ \AA}^{-1}$  (orange curve) provided by VERDI.

concomitantly with the polarized data collection on one side, unpolarized data will be collected on the full detector bank on the other side (VERDI is designed to have  $160^\circ$  horizontal coverage on both sides).

## V. SUMMARY

VERDI is a cold-neutron diffractometer optimized for studies of magnetic and large unit-cell crystal structures with versatility for both powder and single crystal samples and capability for wide-angle XYZ linear polarization analysis. The STS low source frequency of 15 Hz coupled with the appropriate instrument length of 40 m will naturally supply a large single-frame bandwidth of about  $6 \text{ \AA}$  with a wavelength range of  $1 - 6.75 \text{ \AA}$  to achieve the science required wide-range of momentum space. The option to access other wavelength frames or run at half frequency (7.5 Hz) to double the  $Q$ -range accessible for each diffraction angle will provide further flexibility in increasing  $Q$  coverage.

An elliptical guide system with interchangeable guide pieces will provide sufficient flexibility to cover a wide range of incident beam divergences and enabling two modes of operation: a high-resolution / powder configuration with horizontal beam divergence of  $0.2^\circ$  and vertical beam divergence of  $1^\circ$ , or an high-intensity / single-crystal configuration with symmetric beam divergence of  $1^\circ$ . The instrument will include an oscillating radial collimator for background reduction, which will be interchangeable with a supermirror wide-angle polarization analyser on one side of the instrument. A logarithmic

spiral detector design consisting of  $^3\text{He}$  detector tubes, with 3.1 m sample detector distance at forward scattering and 1.2 m at backscattering, supports the science case of high resolution at low- $Q$ . Both sides of the instrument will have full detector coverage in the scattering plane with horizontal angular range of  $5^\circ$  to  $165^\circ$ ). A second row of  $^3\text{He}$  detectors will be added over a  $45-135^\circ$  angular range to provide additional out-of-plane coverage for more efficient non-polarized single-crystal measurements.

VERDI will complement the current diffraction suite at HFIR and SNS facilities by offering longer wavelengths, lower background, higher resolution, and full polarization analysis to provide new inroads into understanding novel small/dilute-moment quantum magnets as well as interactions within extended/molecular orbitals. The unique and versatile characteristics of VERDI will allow growth in areas such as materials synthesis and discovery, energy material investigations and organic material structure analysis.

## ACKNOWLEDGMENTS

The authors gratefully acknowledge the expert advice from I. Zaliznyak, M. Shatruk, J. Paddison, D. Louca, S. Rosenkranz, M. Mourigal, T. M. McQueen, and Raphael Hermann who were directly involved in defining the science requirements for VERDI instrument. This research used resources of the Spallation Neutron Source Second Target Station Project at Oak Ridge National Laboratory (ORNL). ORNL is managed by UT-Battelle LLC for DOE's Office of Science, the single largest supporter of basic research in the physical sciences in the United States.

This manuscript has been authored by UT-Battelle, LLC under Contract No. DE-AC05-00OR22725 with the U.S. Department of Energy. The United States Government retains and the publisher, by accepting the article for publication, acknowledges that the United States Government retains a non-exclusive, paid-up, irrevocable, world-wide license to publish or reproduce the published form of this manuscript, or allow others to do so, for United States Government purposes. The Department of Energy will provide public access to these results of federally sponsored research in accordance with the DOE Public Access Plan (<http://energy.gov/downloads/doe-public-access-plan>).

<sup>1</sup>S. Calder, R. B. K. An, C. R. D. Cruz, M. D. Frontzek, M. Guthrie, B. Haberl, A. Huq, S. A. J. Kimber, J. Liu, J. J. Molaison, J. Neufeind, K. Page, A. M. dos Santos, K. M. Taddei, C. Tulk, and M. G. Tucker, "A suite-level review of the neutron powder diffraction instruments at oak ridge national laboratory," *Rev. Sci. Instrum.* **89**, 092701 (2018).

<sup>2</sup>L. C. Chapon, P. Manuel, P. G. Radaelli, C. Benson, L. Perrott, S. Ansell, N. J. Rhodes, D. Raspino, D. Duxbury, E. Spill, and J. Norris, "Wish: The new powder and single crystal magnetic diffractometer on the second target station," *Neutron News* **22:2**, 22-25 (2011).

<sup>3</sup>M. Mourigal, W. T. Fuhrman, J. P. Sheckelton, A. Wartelle, J. A. Rodriguez-Rivera, D. L. Abernathy, T. M. McQueen, and C. L.

- Broholm, “Molecular quantum magnetism in  $\text{LiZn}_2\text{Mo}_3\text{O}_8$ ,” *Phys. Rev. Lett.* **112**, 027202 (2014).
- <sup>4</sup>Z. Tian, Y. Kohama, T. Tomita, H. Ishizuka, T. H. Hsieh, J. J. Ishikawa, K. Kindo, L. Balents, and S. Nakatsuji, “Field-induced quantum metal–insulator transition in the pyrochlore iridate  $\text{Nd}_2\text{Ir}_2\text{O}_7$ ,” *Nat. Phys.* **12**, 134 (2016).
- <sup>5</sup>Y. Wang, H. Weng, L. Fu, , and X. Dai, “Noncollinear magnetic structure and multipolar order in  $\text{Eu}_2\text{Ir}_2\text{O}_7$ ,” *Phys. Rev. Lett.* **119**, 187203 (2017).
- <sup>6</sup>L. Savary, E. G. Moon, and L. Balents, “New type of quantum criticality in the pyrochlore iridates,” *Phys. Rev. X* **4**, 041027 (2014).
- <sup>7</sup>M. Baum, K. Schmalzl, P. Steffens, A. Hiess, L. P. Regnault, M. Meven, P. Becker, L. Bohaty, and M. Braden, “Controlling toroidal moments by crossed electric and magnetic fields,” *Phys. Rev. B* **88**, 024414 (2013).
- <sup>8</sup>E. Ressouche, M. Loire, V. Simonet, R. Ballou, A. Stunault, and A. Wildes, “Controlling toroidal moments by crossed electric and magnetic fields,” *Phys. Rev. B* **82**, 100408(R) (2010).
- <sup>9</sup>G. M. Espallargas and E. Coronado, “Magnetic functionalities in mofs: from the framework to the pore,” *Chem. Soc. Rev.* **47**, 533 (2017).
- <sup>10</sup>M. Kurmoo, “Magnetic metal-organic frameworks,” *Chem. Soc. Rev.* **38**(5), 1353–1379 (2009).
- <sup>11</sup>O. Fabelo, L. Canadillas-Delgado, I. P. Orench, J. A. Rodriguez-Velamazán, J. Campo, and J. Rodriguez-Carvajal, “Low temperature neutron diffraction studies in  $[\text{Mn}_3(\text{SUC})_2(\text{INA})_2]_n$ : an homometallic molecular 3d ferrimagnet,” *Inorg. Chem.* **50**, 7129 (2011).
- <sup>12</sup>J. A. M. Paddison and A. L. Goodwin, “Empirical magnetic structure solution of frustrated spin systems,” *Phys. Rev. Lett.* **108**, 017204 (2012).
- <sup>13</sup>B. A. Frandsen and S. J. L. Billinge, “Magnetic structure determination from the magnetic pair distribution function (mpdf): ground state of  $\text{MnO}$ ,” *Acta Crystallogr.* **A71**, 325–334 (2015).
- <sup>14</sup>N. Roth, A. F. May, F. Ye, B. C. Chakoumakos, and B. B. Iversen, “Model-free reconstruction of magnetic correlations in frustrated magnets,” *IUCrJ* **5**, 410–416 (2018).
- <sup>15</sup>T. Weber and A. Z. Simonov, “The three-dimensional pair distribution function analysis of disordered single crystals: basic concepts,” *Kristallogr.* **227**, 238–247 (2012).
- <sup>16</sup>I. A. Zaliznyak, A. T. Savici, V. O. Garlea, B. Winn, U. Filges, J. Schneeloch, J. M. Tranquada, G. Gu, A. Wang, and C. Petrovic, “Polarized neutron scattering on hyspec: the hybrid spectrometer at sns,” *J. Phys.: Conf. Series* **862** (2017) 012030 **862**, 012030 (2017).
- <sup>17</sup>P. Willendrup, E. Farhi, E. Knudsen, U. Filges, and K. Lefmann, “Mcstas: Past, present and future,” *J. Neutron Res.* **17**, 35–43 (2014).
- <sup>18</sup>T. Huegle, “Using an onion like neutron scattering instrument model to quickly optimize design parameters,” *Nucl. Instrum. Methods Phys. Res. A* **947**, 162711 (2019).
- <sup>19</sup>J. Lin, H.L.Smith, G. Granroth, D. Abernathy, M.D.Lumsden, B.Winn, A.A.Aczel, M.Aivazis, and B.Fultz, “Mcvine – an object oriented monte carlo neutron ray tracing simulation package,” *Nucl. Instrum. Methods Phys. Res. A* **810**, 86–99 (2016).
- <sup>20</sup>J. Y. Y. Lin, F. Islam, G. Sala, I. Lumsden, H. Smith, M. Doucet, M. B. Stone, D. L. Abernathy, G. Ehlers, and J. F. Ankner, “Recent developments of mcvine and its applications at sns,” *J. Phys. Commun.* **3**, 085005 (2019).
- <sup>21</sup>L. D. Sanjeewa and *et al*, “Competing magnetic ground states of  $\text{naco}_2(\text{seo}_2)_2(\text{oh})$ : A new sawtooth structure with  $\text{Co}^{2+} s = 3/2$ ,” (2022), unpublished.
- <sup>22</sup>B. K. Rai, G. Pokharel, H. S. Arachchige, S. H. Do, Q. Zhang, M. Matsuda, M. Frontzek, G. Sala, V. O. Garlea, A. D. Christianson, and A. F. May, “Complex magnetic phases in the polar tetragonal intermetallic  $\text{NdCoGe}_3$ ,” *Phys. Rev. B* **103**, 014426 (2021).
- <sup>23</sup>S. Nakatsuji, N. Kiyohara, and T. Higo, “Large anomalous hall effect in a non-collinear antiferromagnet at room temperature,” *Nature* **527**, 212 (2019).